

⁵D. Guillon, P. E. Cladis, and J. Stamatoff, *Phys. Rev. Lett.* **41**, 1598 (1978).

⁶R. J. Holden and E. P. Raynes, in *Proceedings of the Seventh International Liquid Crystals Conference*, Bordeaux, France, 1978 (to be published).

⁷The notation was given by D. Forster, T. C. Lubensky, P. Martin, J. Swift, and P. Pershan, *Phys. Rev. Lett.* **26**, 1016 (1971).

⁸M. G. Kim, S. Park, Sr. M. Cooper, and S. V. Letcher, *Mol. Cryst. Liq. Cryst.* **36**, 143 (1976).

⁹T. Yamada and E. Fukuda, *Jpn. J. Appl. Phys.* **12**, 68 (1973).

¹⁰Ch. Gähwiller, *Mol. Cryst. Liq. Cryst.* **20**, 301

(1973).

¹¹See, for example, K. Hossain, J. Swift, J. H. Chen, and T. C. Lubensky, *Phys. Rev. B* **19**, 432 (1979), and references therein.

¹²P. C. Martin, O. Parodi, and P. S. Pershan, *Phys. Rev. A* **6**, 2401 (1973).

¹³W. Helfrich, *Phys. Rev. Lett.* **23**, 372 (1969).

¹⁴Analogies can be drawn to the liquid-vapor transition far away from the critical point where, in spite of the same long-range symmetry properties of the two phases, quantitative differences between the two phases exist.

¹⁵A. F. Martins, A. C. Diogo, and N. P. Vaz, *Ann. Phys. (Paris)* **3**, 361 (1978).

Stimulated Emission of 29-cm^{-1} Phonons in Ruby

P. Hu

Bell Laboratories, Murray Hill, New Jersey 07974

(Received 23 October 1979)

With resonance R_2 laser light pumping, the observation of stimulated emission of the 29-cm^{-1} phonon in ruby is reported. The transverse phonons propagate along the C_3 axis and have some nonlinear gain.

Recently, extensive works have been reported concerning optical generation or detection of single-frequency high-energy phonons.¹⁻⁴ Typically, the generation of these high-frequency phonons was accomplished either by optical excitation through some broad absorption band or the standard technique of a thin heater film. The detector, which is at another part of the same sample, is usually a region where an appreciable amount of ions are maintained at some excited state. In the case of ruby, it is the $\bar{E}(^2E)$ as shown in Fig. 1. The detection of the single-frequency 29-cm^{-1} phonons is then achieved by the observation of time-delayed R_2 light pulses. The delay time corresponds to the time of flight for

phonons to travel ballistically from the generator to the detector. More recently, evidence of high-energy stimulated phonon emission excited by resonant infrared pumping in Al_2O_3 doped with V^{4+} was reported.⁵ I report here the observation of stimulated 29-cm^{-1} phonon emission in ruby with resonant optical pumping based on the frequency and directionality of the phonon observed. Some nonlinear gain is also reported.

A Molelectron UV-400 N_2 laser was used to pump a homemade dye laser with an intracavity prism beam expander. The 5-ns laser pulse had a peak power ~ 10 kW. The linewidth was 0.2 cm^{-1} which was somewhat larger than that of the R_2 line in our ruby samples. The dye laser was then fo-

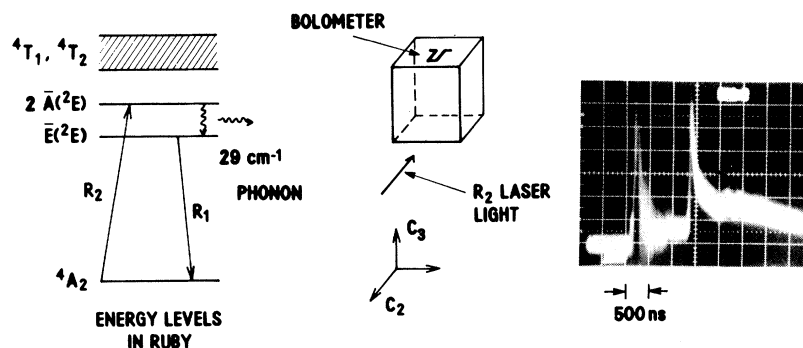


FIG. 1. Schematic energy level diagram in ruby and geometry of the resonance optical excitation experiment. The photograph shows the signals as observed on the scope with a granular aluminum bolometer. The initial and the time-delayed pulses are due to scattered laser light and transverse phonons, respectively.

cused with a 5-cm lens to a spot of diameter ~ 100 μm . Two samples, of Cr concentration 0.03% and 0.05%, respectively, were studied with similar results. The sample dimensions were $1 \times 1 \times 0.5$ cm^3 with the two-fold axis along the shorter dimension. Samples were immersed in liquid helium which was pumped down to 1.6 $^\circ\text{K}$. Half of the sample with the bolometer was enclosed in a light-tight metal box to minimize both scattered laser light and electrical pickup. All surfaces of the crystal were anti-reflection coated. The light propagated along the C_2 axis with polarization normal to the C_3 axis. The phonons propagated along the C_3 axis were detected with a granular aluminum superconducting bolometer. Although many different sizes of bolometers were used, the data presented here were done mostly with a U-shaped bolometer of dimensions 0.75×3 mm^2 with 3 mm along the C_2 axis. The bolometer was biased with milliampere current and an external magnetic field. The linearity of the bolometer was checked by a conventional heater-bolometer experiment and was linear within a few percent. The signals amplified by two $10 \times$ amplifiers can be readily observed on the scope as shown in Fig. 1. In this particular case, the laser spot and the bolometer are aligned along the C_3 axis and the propagation distance is 7.5 mm. The phonon pulses arrived with a velocity $\sim 6 \times 10^5$ cm/sec characteristic of ballistic propagation of transverse phonons. No longitudinal phonon has been observed along the C_3 axis as expected from the selection rules.²

Since the bolometer is a broad-band detector, it is important to prove that the signal is due to the 29-cm^{-1} phonons originating from the $2\bar{A}(^2E)$ level of ruby. The evidences are the following: (1) The signal can only be observed when the dye laser is tuned to R_2 light. The resonance is sharp with a frequency width ~ 0.2 cm^{-1} . (2) When a cw 5145- \AA argon laser was used to excite a small volume between the phonon-generating region and the bolometer, the ballistic phonon signal can almost be eliminated. This is due to the fact that the argon laser will excite an appreciable amount of Cr^{3+} ions to the excited state $\bar{E}(^2E)$. These ions have a very large scattering cross section for the resonant 29-cm^{-1} phonon, and act as a narrow-band absorption filter. Using these techniques, we find that in a carefully prepared sample, the background phonons due to either surface or bulk absorption can be reduced to less than 1% of the signal observed.

By moving the laser excitation spot on the crys-

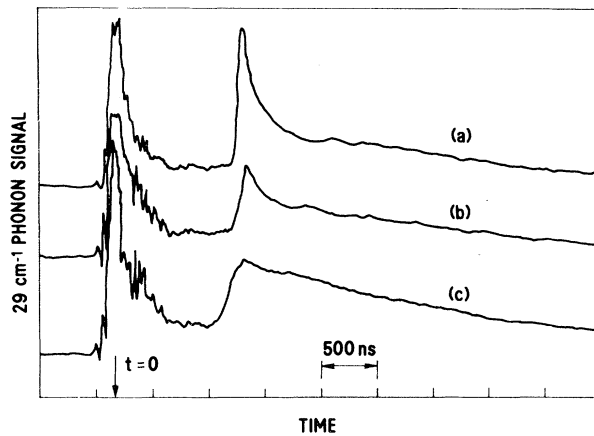


FIG. 2. 29-cm^{-1} phonon signals (linear scale) as a function of time are shown for different geometries. See text.

tal, it is possible to change either the propagation distance or the direction. The arrival time of the signal scales linearly with the distance and therefore confirms that the phonon does propagate ballistically. In Fig. 2(a) the signal is obtained with the bolometer and the laser spot aligned along the C_3 axis and with propagation distance ~ 7.5 mm. Data in Figs. 2 and 3 are obtained by feeding the output of the amplifier to a Biomation transient digitizer connected to a Fabrik-Tek signal averager. Each trace typically is an average of a few thousand laser excitations at a repetition rate of about 50 Hz. The pulse shown in Fig. 2(a) consists of two parts. Most of the leading short pulse (~ 100 -ns width limited by the detector response time) comes from the stimulated 29-cm^{-1} phonon emission. The other part is a microsecond-long 29-cm^{-1} pulse from the spontaneous emission and exhibits a strong phonon bottleneck effect.^{4,6} The directionality of the stimulated emission is best illustrated by Fig. 2(b) which is obtained simply by moving the dye laser 0.7 mm to the side. The short-pulse signal decreases drastically but the long pulse remains essentially intact. The angular half-width of the stimulated emission was measured to be $\sim 6^\circ$. Figure 2(c) was obtained with the dye laser weakly focused (diameter ~ 1 mm) but with the total power remaining constant. In this case, the gain drops drastically but the phonon bottleneck effect persists. This broad pulse, whose pulse width is an order of magnitude longer than to be expected from the finite size of the generator and the detector, also consists of the 29-cm^{-1} phonon but does not have strong directionality. In Fig. 3

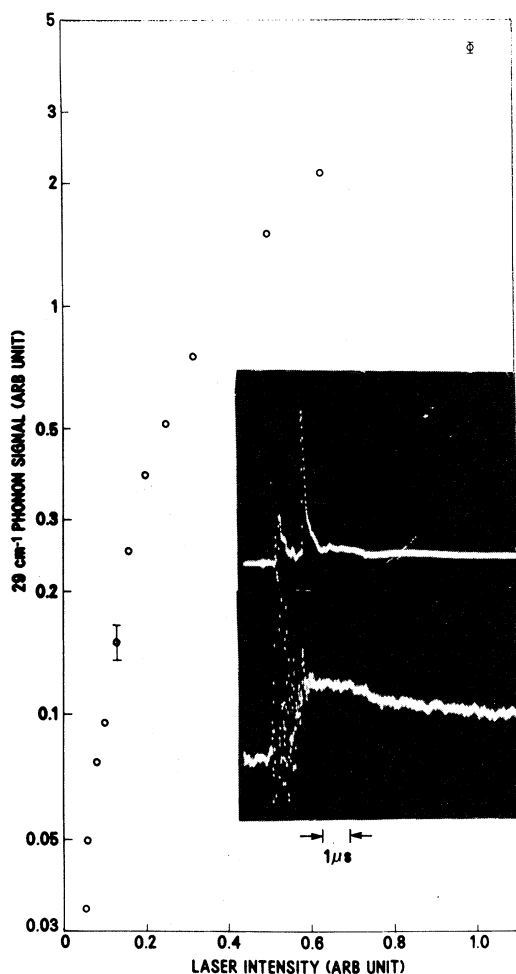


FIG. 3. 29-cm^{-1} phonon signals as a function of input dye-laser power on a semilog plot. Insets are pictures of phonon signal (linear scale) for maximum and $\times\frac{1}{20}$ -dye-laser power, respectively. The vertical gain changes by a factor of 32.

the 29-cm^{-1} short-pulse peak phonon signal is shown as a function of the input dye-laser power. In the inset are two pictures showing the signal at full and $\frac{1}{20}$ dye-laser power, respectively. The gain was increased by a factor of 32 in the lower picture. One of the important features is the relative strength of the short pulse as compared with the long-pulse tail. The tail scales approximately linearly with the dye-laser power but the intensity of the short pulse decreases drastically. The following important experimental features will now be discussed. (1) The pulse consists of two parts. (2) There is nonlinear gain though the data show no threshold or strong exponential gain. (3) The transverse phonon signal propagates along the C_3 axis.

Phonon avalanche and bottleneck effects⁶ have been subjects of extensive study. The qualitative physical picture can be summarized as follows. If there is an initial population inversion, the stimulated phonon emission will be greatly enhanced and will last shorter than a single-ion relaxation time. However, after the inversion is over, the relaxation or the effective lifetime will be much larger than that of a single ion (the bottleneck effect, of the order of 10^4 or more in ruby⁶). The short pulse in our experiment is therefore attributed to stimulated emission, while the long pulse is due to spontaneous emission exhibiting a strong bottleneck effect.

Since the laser power used in our experiment is more than enough to saturate the Cr^{3+} ions in 1 nsec we have an initial population of the order of $5 \times 10^{18}/\text{cm}^3$. The linewidth⁴ and lifetime⁷ of the excited state $2\bar{A}(^2E)$ in ruby are reasonably known. The gain per unit length can then be estimated to be of the order of 10^5 cm^{-1} . The loss is unknown but should be of the order of 1 or less. Though the lifetime will limit the gain length to about $10 \mu\text{m}$, the total gain is still about $e^{(100)}$. Of course, saturation will set in before the gain reaches this order of magnitude, but, nevertheless, we are still in a very high gain regime and this explains the absence of threshold. At the highest laser power, some of the saturation shown in Fig. 3 could also be due to the saturation in the pumping process, namely, half of all the Cr^{3+} ions were excited to the excited state $2\bar{A}(^2E)$. To estimate the total intensity of the stimulated emission, we note that population difference between the two excited states of 2E right after the stimulated emission is small. Therefore the stimulated 29-cm^{-1} phonons should have no problem of escaping from the excited region. The maximum power will therefore be limited by the conversion efficiency of photon to phonon. The maximum power should therefore be of the order of a watt, consistent with our rough estimate from the sensitivity of our detector.

Although the C_3 axis is one of the focusing directions in ruby, the effect for spontaneous emission is small with the geometry ($\sim 1\text{-mm}$ -long excitation length) used.⁸ This is also confirmed in our experiment by the fact that the long pulse shows very little directionality. However, the C_3 axis, being one of the focusing directions, has also the following advantages for the stimulated emission: (a) the two transverse phonons are degenerate; (b) the sound velocity is a minimum; and (c) since the transition probability varies as

$1/v^5$, where v is the velocity of sound, and the velocity of transverse phonon is only half of that of longitudinal phonon, it is therefore not surprising that the transverse mode will dominate if the matrix elements involved are at least comparable. All these factors considered, the experimental facts seem to be quite reasonable.

In summary, I report the observation of stimulated 29-cm^{-1} phonon in ruby. The single-frequency phonons are of transverse mode and propagate along the C_3 axis. Because the background phonons are negligible, the use of a conventional superconducting bolometer with great sensitivity is allowed. This phonon source is in principle tunable by an external magnetic field, and the linewidth is expected to be of the order of 0.02 cm^{-1} .⁴ This intense, directional, tunable high-frequency phonon source may complement the superconducting tunnel junction as an alternative phonon source.⁹

I would like to acknowledge discussions with S. Geschwind, V. Narayanamurti, R. C. Dynes, and C. K. N. Patel. Also I would like to thank T. M. Jedju for technical assistance and M. Chin, who made the granular aluminum bolometers.

⁴K. F. Renk and J. Deisenhofer, *Phys. Rev. Lett.* **26**, 764 (1971); K. F. Renk and J. Peckenzell, *J. Phys. (Paris)*, *Colloq.* **33**, C4-103 (1972); W. Einfeld and

K. F. Renk, *Appl. Phys. Lett.* **34**, 481 (1979).

²A. A. Kaplyanskii, S. A. Bausun, F. A. Rachin, and R. A. Titov, *Pis'ma Zh. Eksp. Teor. Fiz.* **21**, 438 (1975) [*JETP Lett.* **21**, 200 (1975)]; A. V. Akimov, S. A. Basun, A. A. Kaplyanskii, V. A. Rachin, and R. A. Titov, *Pis'ma Zh. Eksp. Teor. Fiz.* **25**, 491 (1977) [*JETP Lett.* **25**, 461 (1977)].

³R. S. Meltzer and J. E. Rives, *Phys. Rev. Lett.* **38**, 421 (1977).

⁴J. I. Dijkhuis, A. van der Pol, and H. W. deWijn, *Phys. Rev. Lett.* **23**, 1554 (1976).

⁵W. E. Bron and W. Grill, *Phys. Rev. Lett.* **40**, 1459 (1978).

⁶J. H. Van Vleck, *Phys. Rev.* **59**, 724, 730 (1941); W. J. Brya and P. E. Wagner, *Phys. Rev.* **157**, 400 (1967); W. J. Brya, S. Geschwind, and G. E. Devlin, *Phys. Rev. B* **6**, 1924 (1972); J. I. Dijkhuis and H. W. deWijn, *Phys. Rev. B* **20**, 1844 (1979).

⁷N. A. Kurnit, I. D. Abella, and S. R. Hartmann, in *Proceedings of the Physics of Quantum Electronics Conference, San Juan, Puerto Rico, 1965*, edited by P. L. Kelley, B. Lax, and P. E. Tannenwald (McGraw-Hill, New York, 1966), p. 267; J. E. Rives and R. S. Meltzer, *Phys. Rev. B* **16**, 1808 (1977).

⁸B. Taylor, H. J. Maris, and C. Elbaum, *Phys. Rev. B* **3**, 1462 (1971); J. Doulat, M. Locatelli, and J. Rivallin, in *Phonon Scattering in Solids*, edited by L. J. Challis, V. W. Rampton, and A. F. G. Wyatt (Plenum, New York, 1976), p. 383; T. Rösch and D. Weis, *Z. Phys. B* **25**, 101 (1976); J. C. Hensel and R. C. Dynes, *Phys. Rev. Lett.* **43**, 1033 (1979).

⁹See, e.g., W. Eisenmenger and A. H. Dayem, *Phys. Rev. Lett.* **18**, 125 (1967); R. C. Dynes and V. Narayanamurti, *Phys. Rev. B* **6**, 143 (1972).

Unified Mechanism for Schottky-Barrier Formation and III-V Oxide Interface States

W. E. Spicer, I. Lindau, P. Skeath, C. Y. Su, and Patrick Chye^(a)

Stanford Electronics Laboratories, Stanford University, Stanford, California 94305

(Received 5 September 1979)

Extensive experimental evidence indicates that the Schottky-barrier formation on III-V semiconductors is due to defects formed near the interface by deposition of the metal (or of oxygen). Detailed level positions are established and assigned to either missing column III or V atoms. This model also applies to formation of states at III-V oxide interface states.

One of the oldest unsolved problems in solid state physics is that of the mechanism of Schottky-barrier (SB) formation (see, for example, Refs. 1-6). An apparently unrelated problem is that of the states formed at the interface between a semiconductor and its oxides. Here, we analyze data of a relatively new type⁷⁻¹⁰ from a large number of metals as well as oxygen-placed GaAs, InP, and GaSb and establish a new mechanism of SB formation. This is based on the formation of defect levels due to the deposition of the foreign

atoms. The same mechanism applies to the states at the III-V semiconductor-metal interface.

A long-standing theory of SB assumes that there are surface states intrinsic to the ideal clean semiconductor.¹¹ These surface states are assumed to remain after application of the metal and to pin the Fermi level—thus, determining the barrier height and device characteristics. For the III-V compounds, this mechanism must be rejected since it has been definitively established¹¹ that there are no intrinsic surface states in the

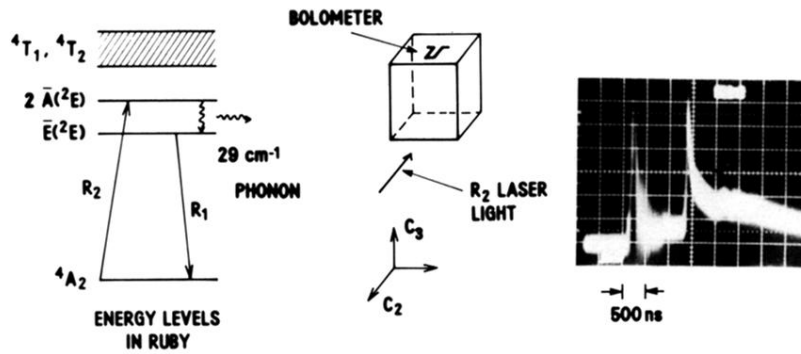


FIG. 1. Schematic energy level diagram in ruby and geometry of the resonance optical excitation experiment. The photograph shows the signals as observed on the scope with a granular aluminum bolometer. The initial and the time-delayed pulses are due to scattered laser light and transverse phonons, respectively.

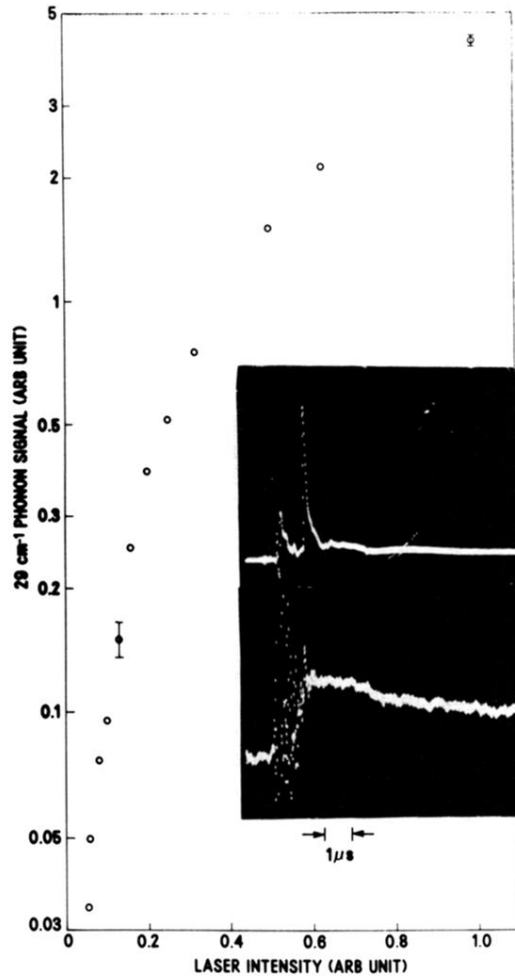


FIG. 3. 29-cm^{-1} phonon signals as a function of input dye-laser power on a semilog plot. Insets are pictures of phonon signal (linear scale) for maximum and $\times\frac{1}{20}$ -dye-laser power, respectively. The vertical gain changes by a factor of 32.